Grain-boundary energies in metals from local-electron-density distributions

John R. Smith
Physics Department, General Motors Research Laboratories, Warren, Michigan 48090-9055

John Ferrante
National Aeronautics and Space Administration, Lewis Research Center, Cleveland, Ohio 44135
(Received 1 March 1985; revised manuscript received 14 April 1986)

The energy contributions of the inhomogeneous electron gas in the vicinity of grain boundaries in *s-p* metals are investigated theoretically. Because there are typically of the order of 10^2 to 10^4 atoms per unit cell in grain-boundary problems, the method of choice typically involves the use of pair potentials, which derive from perturbation theory on a homogeneous electron gas. Since grain boundaries in metals are localized electronic defects, we formulated the problem in terms of perturbation theory on an inhomogeneous electron gas. In that case, we found that the zeroth- and first-order perturbation terms are significant and depend on the local geometric structure of the boundary, unlike the pair-potential approach. Reasonable results were obtained for energies computed to second order for model boundaries in aluminum. A simple, accurate approximation was found for the zeroth- and first-order terms. The sum of the second-order and Ewald-like terms can also be approximated in a pair-potential-like form which depends on the average of the electron densities seen by the atoms in the pair. This suggests a viable approach for computing the grain-boundary structure and energy which is presumably more accurate than the usual pair-potential method.

I. INTRODUCTION

The determination of the nature and properties of grain boundaries in metals has been a long-standing problem in materials science.[1-4] Grain boundaries can exert a profound effect upon mechanical, chemical, and electronic properties. For example, boundaries affect the motion of dislocations and hence influence mechanical strength. Fast-diffusion short circuiting occurs along grain boundaries causing diffusional creep. Chemical segregation occurs at boundaries promoting intergranular corrosion and brittleness. Coercivity in magnetic materials has been observed[5] to depend on grain size.

How does one calculate the structure and energetics of grain boundaries? Because actual grain boundaries contain of the order of 10^2 to 10^4 atoms per unit cell, this question has not been seriously addressed via first-principles solid-state methods. Rather, the method of choice has been, of necessity, that of pair potentials (see, e.g., Refs. 6–12). Recently, we and others have developed self-consistent methods for computing total energies from first principles for simple defects in transition[13] and *s-p* metals.[14]

In the following, we would like to present the first calculation of grain-boundary energies to go beyond the usual pair-potential approximation. That is, electron-density profiles in the boundary and corresponding electronic total energies are computed self-consistently for a model grain boundary appropriate to simple metals such as aluminum. An unexpected finding was that these electronic contributions can be accurately computed via a simple procedure. This suggests that a new method may be viable for determining structures and energies of defects like grains boundaries in *s-p* metals.

In Sec. II we first discuss a perturbation expansion for computing grain-boundary energies in *s-p* metals beyond the pair-potential approximation. Then we introduce a model grain boundary in aluminum which is designed to allow a simple estimate of the size of electronic contributions to grain-boundary energies. In Sec. III this estimate is carried out and results are given. The discovery of a simple, accurate approximation for computing electronic contributions to grain-boundary energies is discussed. The success of this approximation scheme allows us to suggest, in Sec. IV, a new method for computing structures and energies of grain boundaries. Concluding remarks are found in Sec. V.

II. MODEL AND FORMALISM

The total energy E_G of an *s-p* metal with grain boundary can be written as

$$E_G = E^*_{\text{Ewald}} + E^*_0[n_c] + E^*_1[n_c;\delta V_c] + E^*_2[n_c;\delta V_c] + \cdots , \tag{2.1}$$

where the asterisks are added because the perturbation is done on a homogeneous electron gas, n_c is the electron density of the homogeneous unperturbed system, E^*_{Ewald} is the Ewald electrostatic energy,[11] the subscripts of E^* indicate successively higher orders of the perturbation δV_c, and δV_c is the difference between an array of pseudopotentials for a crystal with grain boundary and the potential of the unperturbed (homogeneous) system. These pseudopotentials may be nonlocal or local. If one terminates the expansion at $E^*_2[n_c;\delta V_c]$ one finds that[11]

$$E_G \cong F(n_c) + \tfrac{1}{2}{\sum_{l,l'}}' V_{ll'}(n_c) , \tag{2.2}$$

where $V_{ll'}(n_c)$ is a pairwise interaction between sites l and l', the prime on the summation excludes the $l=l'$ term, and $F(n_c)$ is a structure-independent energy.

Carlsson[15] calls situations for which Eq. (2.2) is appropriate "constant-volume" problems for which only a relatively small heterogeneity is found on a local scale. An appropriate example might be the prediction of phonon-dispersion curves. He labels situations where the heterogeneity is substantial, such as at surfaces and vacancies, as "bond-breaking" problems. He found bond-breaking problems to be not well represented by a second-order perturbation approximation.

What about grain boundaries? An example of a grain boundary is shown schematically in Fig. 1. This particular example shows a symmetric "tilt" boundary for which one grain is rotated with respect to the other by the misorientation angle θ around the tilt axis which is normal to the plane of the figure. In general, of course, the rotation axis, the misorientation angle, and also the inclination of the plane of the boundary can be varied arbitrarily. Electron micrographs of grain boundaries in aluminum, for example, can be found in Ref. 12.

The heterogeneity is not so substantial as at a free surface but is large enough that one might question whether they fall in Carlsson's constant-volume situation. Indeed, Wolf's[9] results suggest that they do not.

How would one go about improving upon Eq. (2.2)? One way would be to include third- and higher-order perturbation terms in Eq. (2.1). That would make it necessary to take into account three-, four-, and perhaps higher-particle interactions, a significant complication.[16,17] An alternative approach would be to employ a perturbation expansion on an *inhomogeneous* electron gas:

$$E_G = E_{\text{Ewald}} + E_0[n_0(\mathbf{r})] + E_1[n_0(r);\delta V] + E_2[n_0(\mathbf{r});\delta V] + \cdots . \quad (2.3)$$

The electron density $n_0(\mathbf{r})$ is a starting distribution which is as close as is convenient to that of the crystal *with* grain boundary. That is, $n_0(\mathbf{r})$ is an approximation to the exact density distribution for the crystal with grain boundary which is more easily computed than is the exact solution. The potential δV is the difference between an array of pseudopotentials of the crystal with grain boundary and the potential used to compute $n_0(\mathbf{r})$. Again, these pseudopotentials may be nonlocal or local. Because $n_0(\mathbf{r})$ is closer to the exact electron density than n_c is, one would expect Eq. (2.3) to be more accurate than Eq. (2.2) when both expansions are truncated at the same order in the perturbation. This kind of approach was used with some success earlier by the authors[14] to compute bimetallic adhesion energies. There it was found that one could truncate the perturbation expansion Eq. (2.3) at $E_1[n_0(\mathbf{r});\delta V]$ and still obtain reasonable accuracy. Note that in Eq. (2.3) $E_0[n_0(\mathbf{r})]$ and $E_1[n_0(\mathbf{r});\delta V]$ will depend on the local geometric structure of the boundary. This is in contrast to $E_0^*[n_c]$ and $E_1^*[n_c;\delta V_c]$ of Eq. (2.1) which do not depend on structure.

In analogy with our bimetallic adhesion calculations, we will assume that n_0 can be taken to be only a function of y, the coordinate perpendicular to the grain boundary. Remember, this is not the actual electron density but a one-dimensional approximation to it, taken as close as possible to the exact density to aid convergence of the perturbation expansion, Eq. (2.3). We will use this to estimate grain-boundary energies and their energy components in aluminum.

Later, in Sec. IV, we will discuss a method for computing electronic contributions to grain-boundary energies which will allow treatment of fully three-dimensional, nonplanar starting electron-density distributions $n_0(\mathbf{r})$. This will presumably lead to higher accuracy in determining atomic positions.

Because for now we are assuming n_0 to be only a function of y, we can form the pseudopotential used to compute $n_0(y)$ from a stepped-jellium model[14,18] by averaging the atom density parallel to the boundary, forming a homogeneous slab of volume-averaged atom density n_B for the core which is sandwiched within the host crystalline material of the grains of volume-averaged atom density n_H. The boundary core is the region of material in which the atomic coordination differs from that of the perfect crystal. In general, this region has been found to be quite narrow in metals and to have a density lower than that of the perfect crystal. The lower density is due primarily to the inability of the system to achieve efficient atomic packing in the transition region between the crystals adjoining the boundary. We will take values of boundary width and n_B/n_H from experiment and the results of previous model calculations. Direct observation by field ion microscopy[19] and electron microscope lattice imag-

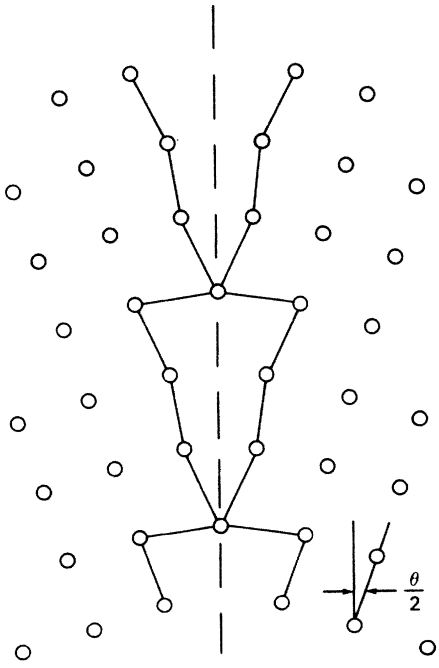

FIG. 1. An example of a grain boundary shown in cross section. Two grains are intersecting at an angle, forming a tilt boundary. The atoms in the core of the grain boundary are joined by the heavy lines. The edge of a plane through the center of the grain boundary is shown as the dashed line.

ing[20] shows that this width in the metals investigated is narrow, i.e., less than about two nearest-neighbor distances wide (10—11 a.u.). The length of relrods in reciprocal space produced by grain-boundary diffraction[21] indicates a width $\simeq$13 a.u. However, this width refers to the region near the boundary which is significantly stressed by relaxations in the boundary and which is wider than the width of the region of significantly lower density. Measurements of fast grain-boundary "short-circuit" diffusion indicate a width $\sim$6—13 a.u.

A considerable body of information indicates that the introduction of a boundary produces an expansion normal to the boundary plane, as mentioned earlier. Values of n_B/n_H are obtained by distributing this expansion uniformly over the boundary width taken to be 10 a.u., as discussed previously. Hard-sphere rigid-lattice models of a variety of grain boundaries in Ref. 22 predict values of n_B/n_H in the range 0.75—0.90. However, these values are clearly too small since they do not allow for boundary relaxation. Values of n_B/n_H obtained from molecular statics calculations using pairwise interatomic potential models indicate $n_B/n_H=0.88$ as the average for a variety of [110] tilt boundaries[23] and $n_B/n_H=0.83$ as the average for a variety of [100] tilt boundaries[24] in Al. $n_B/n_H=0.90$ is the estimated average for several [100] twist boundaries[9] in Al and $n_B/n_H=0.94$ and 0.90 for a variety of [100] twist boundaries[25] in Cu and Ni, respectively. Unfortunately, only a few experimental measurements are available. The value $n_B/n_H=0.96$ is obtained[26] from measurements on a $\Sigma=3$ tilt boundary parallel to $(1\bar{2}1)$ in Al, $n_B/n_H=0.94$ is obtained[27] for a $\Sigma=11$ tilt boundary parallel to (113) In Au, and $n_B/n_H=0.83-0.89$ is estimated[28] for a high angle [100] twist boundary in Au.

Now let us return to a discussion of the calculational method. The difference δV between the actual atomic array of pseudopotentials and the stepped-jellium starting potential referred to above could be included in perturbation theory for the total energy [Eq. (2.3)].

The electron density $n_0(y)$ is determined from the self-consistent solution of the Kohn-Sham[29] equations of the form (atomic units are used throughout the paper unless noted otherwise)

$$\left[-\frac{1}{2}\frac{d^2}{dy^2}+v_{\rm eff}(n_0;y)\right]\Psi_k^{(i)}(y)=\tfrac{1}{2}(k^2-k_F^2)\Psi_k^{(i)}(y)\ ,$$

$$n_0(y)=\frac{1}{4\pi^2}\sum_{i=1}^{2}\int_0^{k_F}dk\ |\Psi_k^{(i)}(y)|^2(k_F^2-k^2)\ , \qquad (2.4)$$

$$v_{\rm eff}(n_0;y)=\phi_0(y)+\frac{\delta E_{\rm xc}[n_0(y)]}{\delta n_0(y)}\ ,$$

with Poisson's equation

$$\frac{d^2\phi_0(y)}{dy^2}=-4\pi[n_0(y)-n_+(y)]\ , \qquad (2.5)$$

where $E_{\rm xc}[n_0(y)]$ is the electronic exchange-correlation energy, $n_+(y)$ is the stepped-jellium density distribution, $\Psi_k^{(i)}(y)$ are the doubly degenerate electron wave functions, and $k_F^2/2$ is the Fermi energy.

III. ELECTRONIC CONTRIBUTIONS TO THE GRAIN-BOUNDARY ENERGY

Having solved Eqs. (2.4)—(2.5) self-consistently for $n_0(y)$ (Fig. 2), we are now in a position to calculate total energies for grain boundaries in aluminum. The electron kinetic energy component of $E_0[n_0(y)]$ in Eq. (2.3) is given by

$$A\sum_{\substack{k,k_x,k_z\\({\rm occ})}}\int dy\{(k^2+k_y^2+k_z^2)|\Psi_k^{(i)}(y)|^2 +[v_{\rm eff}(n_0;\pm\infty)-v_{\rm eff}(n;y)]n_0(y)\}\ . \qquad (3.1)$$

The grain-boundary energy σ_G is given by

$$\sigma_G=(E_G-E_c)/A\ , \qquad (3.2)$$

where A is the cross-sectional area of the grain-boundary interface and E_c is the total energy of perfect crystal. Combining Eqs. (2.3) and (3.1) with (3.2) we find a kinetic energy contribution to σ_G of -6596 erg/cm^2. The negative sign indicates that the electron kinetic energy is lowered by the introduction of a grain boundary. This is consistent with the volume-averaged electron density in the boundary core being less than in the single crystal. The value is also an order of magnitude larger than typical values of σ_G (see below). The exchange-correlation en-

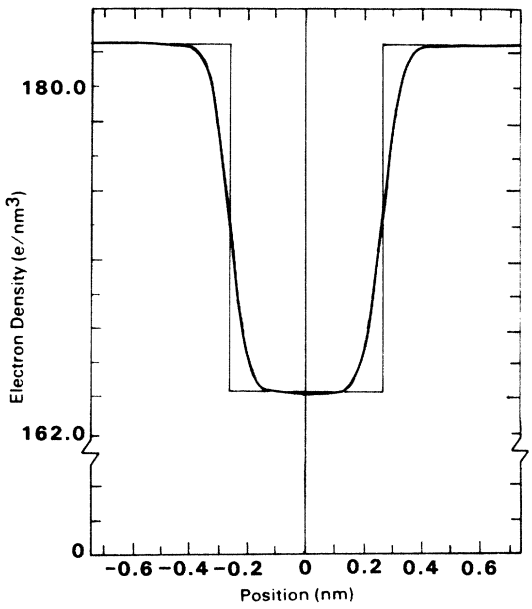

FIG. 2. Self-consistent planar-averaged electron density plotted as a function of position along a line perpendicular to a grain boundary in aluminum (e.g., perpendicular to the dashed line in Fig. 1). The electron density in the bulk of the grain is Zn_H, where Z is the valence of aluminum (=3) and n_H is the volume-averaged atom density of single-crystal aluminum. The boundary density $n_B=0.9n_H$. The width of the grain (indicated by the distance between steps in the figure) is taken to be 10 a.u.=0.53 nm.

ergy density is evaluated in terms of the local electron density,[18,29] and its contribution to σ_G is also large, 2980 erg/cm^2. The sign is also consistent with the electron density in the core being lower than in the grain.

Clearly it would be important to include these energy components in grain-boundary energy calculations. But it is a tedious precursor indeed to have to solve Eqs. (2.4)—(2.5) self-consistently in order to obtain these and the other terms in Eq. (2.3).

Our results for $n_0(y)$ in Fig. 2 suggest a different approach, however. Note first that the Friedel-like oscillations which were evident in the earlier adhesion calculations[14] are very weak here. This is presumably because we have a relatively mild drop in planar-averaged electron density in going through the grain boundary. Secondly, while the boundary is only just over 5 Å wide, the electron density in the boundary is approximately equal to Zn_B over much of the width, where Z=valence of Al (=3). This is a manifestation of short screening lengths in metals. Thus, we have a localized electronic defect. This also suggests a step-density approximation. That is, we approximate $n_0(y)$ as a uniform density in the core equal to Zn_B and as a uniform density in the grain equal to Zn_H. Not only does this bypass Eqs. (2.4)—(2.5), but also this makes the computation of E_G simple [Eq. (2.3)], because the homogeneous electron gas energy density is a simple functional[11,30—32] of n_0. Thus in the step-density approximation,

$$E_G \cong V_B \rho_B f(\rho_B) + V_H \rho_H f(\rho_H) , \tag{3.3}$$

where V_B is the volume of the boundary core, V_H is the volume of the grains, $\rho_H = Zn_H$, $\rho_B = Zn_B$, and

$$f(n) = -\frac{\beta}{2}\left[\frac{4\pi Z^2}{3}\right]^{1/3} n^{1/3} + \tfrac{3}{10}(3\pi^2)^{2/3} n^{2/3} - \frac{3}{4}\left[\frac{3}{\pi}\right]^{1/3} n^{1/3} - \frac{0.056 n^{1/3}}{0.079 + n^{1/3}} + \sum_{\mathbf{k}} \langle \mathbf{k} \mid \delta V \mid \mathbf{k} \rangle + \frac{n}{Z^2} \sum_{\mathbf{q}\,(\neq 0)} |S(\mathbf{q})|^2 F(q) . \tag{3.4}$$

The first term on the right-hand side of Eq. (3.4) is due to the Ewald term, E_{Ewald}. The factor β is close to 1.8 and depends on the crystal structure. The second term is due to the electron kinetic energy, the third to electron exchange, and the fourth to electron correlation. The fifth and sixth terms are due to the first (E_1) and second (E_2) order perturbation terms, respectively. When the Ashcroft[30] pseudopotential with a core radius r_c^* is used, the first-order perturbation term becomes $2\pi n r_c^{*2}$. Simple expressions can also be derived for other, nonlocal pseudopotentials if desired. The structure factor $S(\mathbf{q})$ is given by

$$S(\mathbf{q}) = N^{-1} \sum_j \exp(-i\mathbf{q}\cdot\mathbf{R}_j) , \tag{3.5}$$

where the sum is over the N atoms of the unit cell. For a crystalline, Bravais lattice, $S(\mathbf{q}) = \delta_{\mathbf{q},\mathbf{K}}$, $\mathbf{K}$ being a reciprocal-lattice vector. The energy-wave-number characteristic $F(q)$ has been evaluated for nonlocal pseudopotentials (see, e.g., Ref. 31). For a local pseudopotential, it has the form[32]

$$F(q) = \tfrac{1}{2}\chi_H^{(1)}(q) \mid v^{\text{ion}}(q) \mid^2 , \tag{3.6}$$

where

$$\chi_H^{(1)}(q) = \frac{q^2}{4\pi}\left[\frac{1}{\epsilon(q)} - 1\right] , \tag{3.7}$$

and $\epsilon(q)$ is the static dielectric function.[32—34] For this estimate of grain-boundary energy components we have chosen to use the Ashcroft[30] pseudopotential, where

$$v^{\text{ion}}(q) = -\frac{4\pi Z}{q^2}\cos(qr_c) . \tag{3.8}$$

Since E_1 depends on $v^{\text{ion}}(q)$ as $q \to 0$ and E_2 on q values at the reciprocal-lattice vectors, the same value of core radius may not be appropriate for these two terms. Here $r_c = 1.12$ a.u. was obtained from fits to Fermi-surface data. We found that $r_c^* = 1.221$ a.u. yields a minimum in the total energy of the Al crystal at the experimental lattice constant (see also Ref. 32). For this estimate we compute the local energy density associated with the Ewald term via a fcc structure, so that[11] $\beta = 1.791\,75$. The local lattice constant of the fcc structure is chosen to reflect the local atom density (n_B or n_H in the step-density approximation). For consistency, the same structure is used for the local energy of the second-order perturbation term. Because this assumes a higher degree of commensuration than exists in the actual boundary, this presumably underestimates the grain-boundary energy somewhat but will perhaps suffice for an estimate. Again, in Sec. IV we will indicate how one might treat more general, inhomogeneous structures.

As a test of the accuracy of our model for bulk properties, we computed the bulk modulus. Our calculated value of 0.661 N/m^2 compares reasonably well with an experimental value[35] for aluminum of 0.722×10^{11} N/m^2.

We can now test Eq. (3.3) by comparing values of electron kinetic and exchange-correlation energies obtained from it with the values we obtained earlier by solving Eqs. (2.3)—(2.5) and (3.1) and (3.2). One can see from Table I that Eq. (3.3) yields quite accurate answers.

TABLE I. Electron kinetic and exchange-correlation energy contributions to the Al grain-boundary energy. The grain-boundary core width is 10 a.u. The results are given for two volume-averaged boundary densities n_B. The quantity n_H is the volume-averaged atom density of crystalline Al. The self-consistent method refers to the solution of Eqs. (2.3)—(2.5) and (3.1) and (3.2), while the step-density method to Eqs. (3.2)—(3.4).

Boundary densities n_B/n_H	Method	Energy components (erg/cm^2) Kinetic	Exchange correlation
0.9	Self-consistent	−6596	2980
0.9	Step density	−6597	3005
0.73	Self-consistent	−154 97	7262
0.73	Step density	−149 68	7069

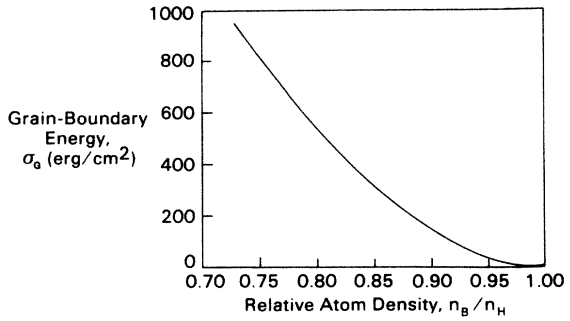

FIG. 3. Grain-boundary energy in aluminum as a function of the ratio of the volume-averaged atom density in the boundary, n_B, to the volume-averaged atom density in the host crystal, n_H. The grain-boundary energy σ_G was approximated as via Eqs. (3.2) and (3.3). The width of the boundary is 10 a.u.

One might wonder if Eq. (3.3) would have such accuracy throughout the physically reasonable range of n_B/n_H. From the discussion above Eq. (2.4) of the expected range of n_B/n_H, one might expect that $n_B/n_H=0.73$ to be just below the lower limit of the range. Thus we repeated that calculation for 0.73, and the results are shown in Table I. While both kinetic and exchange-correlation energies have increased in size and the absolute error has increased correspondingly, the latter is nevertheless smaller than 3.5%.

This accuracy allows us to use Eqs. (3.3) and (3.2) to easily estimate σ_G as a function of n_B/n_H. The result is shown in Fig. 3. For the range of $0.83 \leq n_B/n_H \leq 0.94$, we find 51 erg/cm$^2 \leq 400$ erg/cm^2. These results are consistent with measurements of average-grain-boundary energies in aluminum[36] of 324 erg/cm^2 at 450°C and[37] 340 erg/cm^2 at 380°C. The estimate[36] $d\sigma_G/dT=-0.12$ erg/cm^2°C implies that $\sigma_G \cong 411$ erg/cm^2 at 0 K.

The components of the grain-boundary energy are shown in Fig. 4. We see immediately that each of the components is much larger than the total grain-boundary energy σ_G. The energy contributions from the usual approach, Eqs. (2.1) and (2.2), are distributed over the various orders of the perturbation in a different manner than in Eq. (2.3), the present method. Because $n_0(y)$ is closer to the exact $n(\mathbf{r})$ than is n_c, the lower-order terms in Eq. (2.3) (and Fig. 4) effectively contain contributions from higher-order terms in Eq. (2.1). It is this sort of an effect that led to useful results in adhesion calculations[14] with the exclusion of terms of order higher than $E_1[n_0(\mathbf{r});\delta V]$. As noted earlier, E_0 and E_1 in principle depend on the boundary structure, while E_0^* and E_1^* do not.

In Fig. 4 it is clear that the second-order (E_2) energy is much smaller than the first-order (E_1) energy. However, it is not small relative to the total grain-boundary energy σ_G. This was not true for face-dependent-surface energies of aluminum,[38] and was presumably not true for the surface energy and bimetallic adhesive energy calculations discussed earlier.[14] Why is that? In a grain boundary we find a fundamentally different situation than we have in cleavage in the sense that the grain-boundary core is a region in space whose average atomic density is different from that of the crystal. That is, in creating the grain boundary we have in the core a segment of the solid whose energy density is different from the crystal. As the core region thickens, it can be thought of as having a "bulk" energy density and an energy density associated with the interface between the core and the host crystal. On the other hand, in cleavage the corresponding interface is between crystal and vacuum, and so in cleavage there is no corresponding bulk or core energy density. In fact this basic difference affects all the energy components.

Now Eq. (3.3) is appropriate for estimating electron contributions to the grain-boundary energy and, in fact, the total grain-boundary energy is given with reasonable

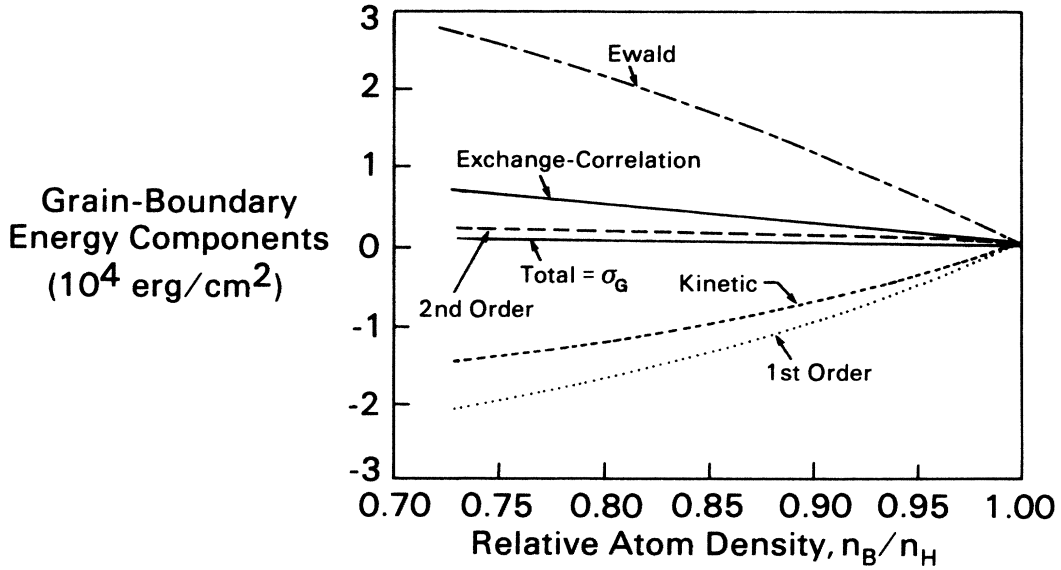

FIG. 4. Grain-boundary energy components in aluminum as a function of the ratio of the volume-averaged boundary atom density n_B to the volume-averaged atom density in the host crystal, n_H. See Eqs. (2.3), (3.3), and (3.34). The width of the boundary is 10 a.u.

accuracy. Certain improvements suggest themselves, however. As indicated in Table I, Eq. (3.3) is an excellent approximation for kinetic and exchange-correlation components. The E_{Ewald} and E_2 terms are nonlocal in nature and require further consideration. An approximation like Eq. (3.3) is adequate for E_{Ewald} and E_2 for interactions within the core or within the crystallite but treats interaction across the interface between the core and the crystallite in an average way which does not accurately account for detailed geometry effects in the interface which are important if one is interested in computing atomic positions via energy minimization. The generalization of Eq. (3.3) to go beyond that model in order to determine grain-boundary structure is straightforward and introduced in the next section.

IV. NONLOCAL EFFECTS

From the preceding discussion it would seem desirable for computing atomic positions in the interface to go beyond Eq. (3.3), particularly for the parts of the E_{Ewald} and E_2 components associated with interactions across the interface. We first write the second-order energy term in the following form, where for simplicity of presentation we have assumed a local perturbation $\delta V(\mathbf{r})$:

$$E_2[n_0(\mathbf{r});\delta V(\mathbf{r})]=\tfrac{1}{2}\int d\mathbf{r}_1\int d\mathbf{r}_2\,\delta V(\mathbf{r}_1)\delta V(\mathbf{r}_2)\times\chi^{(1)}[n_0(\mathbf{r});\mathbf{r}_1,\mathbf{r}_2]\,, \tag{4.1}$$

where $\chi^{(1)}[n_0(\mathbf{r});\mathbf{r}_1,\mathbf{r}_2]$ is a (nonlocal) response function for an inhomogeneous solid of electron-density distribution $n_0(\mathbf{r})$. As an example of such a response function, in Ref. 39 one is given for a jellium surface. Because here we must deal with the order of 10^2 to 10^4 atoms per unit cell, we must look for a relatively simple means of approximating Eq. (4.1). Chakravarty *et al.*[40] found that the following approximation led to accurate results for the hydrogen molecule:

$$\chi^{(1)}[n_0(\mathbf{r});\mathbf{r}_1,\mathbf{r}_2]\cong\chi_H^{(1)}\left[\frac{n(\mathbf{r}_1)+n(\mathbf{r}_2)}{2};|\,\mathbf{r}_1-\mathbf{r}_2\,|\right]. \tag{4.2}$$

That is, the response function for the inhomogeneous system is approximated by that of a homogeneous system at the average of the densities $n(\mathbf{r}_1)$ and $n(\mathbf{r}_2)$. This same approximation was also found to yield reasonable results for metal surface energies.[38,41]

This suggests that the contribution to $E_2[n_0(\mathbf{r});\delta V(\mathbf{r})]$ of, say, atoms 1 and 2 can be written in terms of a pair-potential-like term evaluated at the density $[n(\mathbf{r}_1)+n(\mathbf{r}_2)]/2$.

That is, one might presume the following expression would be more accurate than Eq. (3.3):

$$E_G\cong\int n_0(\mathbf{r})\varepsilon[n_0(\mathbf{r})]d\mathbf{r}+\tfrac{1}{2}{\sum_{l,l'}}'V_{ll'}\left[\frac{n_l+n_{l'}}{2}\right], \tag{4.3}$$

where

$$\varepsilon[n_0]=f(n_0)-\frac{1}{Z}\sum_{l'\,(\text{hom.})}V_{1l'}(n_0)\,. \tag{4.4}$$

Here $f(n_0)$ is given by Eq. (3.4) and is evaluated for any single-crystal structure which is convenient. The term $-(1/Z)\sum_{l'}V_{1l'}(n_0)$ must be evaluated for the same crystal structure used for $f(n_0)$.

Equation (4.4) is based on a local, homogeneous-density approximation to $\varepsilon[n_0(\mathbf{r})]$ as suggested by the accuracies exhibited in Table I. That is, it is computed via Eq. (4.4) for a homogeneous system. The purpose of writing $\varepsilon[n_0]$ as a difference between a total energy density $[f(n_0)]$ and a pair-energy density is to include the structure-independent term which arises when writing E_2^* in terms of a pair potential.[42,43] The remainder of the total energy is in the form of a nonlocal, pairlike term.

Several comments are in order. First, Eqs. (4.3) and (4.4) retain the local, "bulk" energy contribution to E_2 coming from the core atom density being lower than that in the crystallite. This was also in the expression, Eq. (3.3), as discussed in Sec. III. Secondly, the pairlike term

$$\tfrac{1}{2}\sum_{l,l'}V_{ll'}\left[\frac{n_l+n_{l'}}{2}\right]$$

is more complicated than the usual pair interaction because of the density dependence. However, density-dependent pair potentials are well known[32] and the added effort is trivial. Third, $n_0(\mathbf{r})$ could be obtained from a linear superposition of atomic electron-density distributions. It would be preferable to use atomic densities computed from pseudopotentials for this because of their relatively smooth nature. Note, we would find $\int n_0(\mathbf{r})\varepsilon[n_0(\mathbf{r})]d\mathbf{r}$ to be structure dependent, unlike $E_0^*[n_c]$ and $E_1^*[n_c;\delta V_c]$ of Eq. (2.1). This structure dependence comes from doing perturbation theory on an inhomogeneous electron gas $n_0(\mathbf{r})$. An even simpler though presumably less accurate $n_0(\mathbf{r})$ would be the step-density distribution discussed above Eq. (3.3). Even with the step-density approximation, Eq. (4.3) would be expected to be more accurate than Eq. (3.3) because Eq. (4.3) allows direct incorporation of the actual three-dimensional geometric structure of the boundary.

The energies $\varepsilon[n_0]$ are easily tabulated[11] as a function of (homogeneous) density n_0, and this needs to be done only once for each metal. Then for each (three-dimensional) grain-boundary structure,

$$\int n_0(\mathbf{r})\varepsilon[n_0(\mathbf{r})]d\mathbf{r}$$

is simply determined from the tabulation. Thus the grain-boundary energy E_G may be determined from Eq. (4.3) for each structure with little more effort than that required for the usual pair-potential calculation.

The pair term in Eq. (4.3) is given in terms of the pseudopotential by[11,32]

$$V_{ll'}(n_{ll'})=\frac{Z^2}{R_{ll'}}+\frac{1}{\pi^2}\int_0^\infty dq\,\frac{q}{R_{ll'}}F(q,n_{ll'})\sin(kR_{ll'})\,, \tag{4.5}$$

where $R_{ll'}\equiv|\,\mathbf{R}_l-\mathbf{R}_{l'}\,|$ and $n_{ll'}\equiv(n_l+n_{l'})/2$. For a local pseudopotential, $F(q)$ is given by Eq. (3.6). Plots of

$V_{ll'}(n_{ll'})$ as a function of $R_{ll'}$ for various choices of pseudopotential and density can be found in numerous references (see, e.g., Ref. 32).

That completes the description of our approach based on perturbation theory of a nonuniform electron gas. Now, we would like to make a few comments. First, this is the first time to our knowledge that electronic energies associated with a localized electronic defect such as a grain boundary have been computed beyond the usual pair-potential approximation. Secondly, empirical pair potentials have been used for grain-boundary-structure calculations, and one might wonder how empirical information might enter here. For a given structure, the total energy in the preceding equations is determined once one specifies the pseudopotential. Thus empirical information must enter via the pseudopotential, rather than entering via a pair potential. So empirical information can be used as in other methods if desired.

Finally, it is perhaps useful to compare our Eq. (4.3) with the more standard approaches. See, e.g., Ref. 10. The usual approximation is to write the energy as

$$E_G \cong PV + \tfrac{1}{2}\sum_{l,l'}{}' V_{ll'} , \tag{4.6}$$

where P is described as a Cauchy pressure. On comparing Eq. (4.6) to Eq. (4.3), one sees that they are of similar form with PV in the earlier expression [Eq. (4.6)] being replaced by

$$\int n_0(\mathbf{r})\varepsilon[n_0(\mathbf{r})]d\mathbf{r}$$

in our Eq. (4.3) and with the pair potential $V_{ll'}$ being replaced by the pairlike term $V_{ll'}(n_{ll'})$. One could derive the PV term as follows. Assume that the boundary region is homogeneous and do an expansion of the energy of the boundary region in powers of the volume, keeping only the linear term. Then the pressure P is obtained from a volume derivative of the energy of a homogeneous system. This could be considered as a linear approximation to our Eq. (4.3), with the following limitations. First, $V_{ll'}$ must be determined from the same pseudopotential [Eq. (4.5)] used to obtain P and the site-site density dependence $n_{ll'}$ suppressed. Secondly, to avoid double counting in the computation of P, the pair interaction energy for a homogeneous system should be subtracted from the energy [as we did in Eq. (4.4)] prior to taking the volume derivative. Finally, our Eq. (4.3) is derived from perturbation theory on an inhomogeneous electron gas, while Eq. (4.6) presumes the unperturbed electron gas to be homogeneous. Since a grain boundary in a metal is a local electronic defect, an inhomogeneous starting electron-density distribution which mimics the local defect would be expected to be closer to the exact density distribution than would a homogeneous starting density distribution. Thus one would expect Eq. (4.3) to have greater accuracy than Eq. (4.6).

V. SUMMARY

We formulated the total energy of an s-p metal with a grain boundary in terms of a perturbation theory on an inhomogeneous electron gas. This is to be contrasted with the usual pair-potential approach which is derived from perturbation theory on a homogeneous electron gas. Since a metallic grain boundary is a localized electronic defect, greater accuracy can be expected from a starting electronic distribution which is locally inhomogeneous.

It turns out that grain-boundary energies can in fact be computed in this way without resorting to the usual pair-potential approximation. The unperturbed electron-density distribution was first obtained from a fully self-consistent, quantum-mechanical calculation using a stepped-jellium model in analogy with our earlier[14] bimetallic adhesion calculations. We found that unlike the usual pair-potential calculation, the zeroth- and first-order perturbation terms were significant and depended on local geometry in the boundary. We discovered a simple and accurate approximation for the energy components. With it, one can write the electronic energy density at a point in the boundary in terms of the electronic energy density of a homogeneous metal whose atom density is the same as the local atom density. We used this approximation to compute all of the energy components for the model boundary as a function of the boundary atom density. It was clear from those results that all components of these electronic contributions are large over a broad range of boundary densities.

The success of this approximation suggested a way to compute energies and structures of grain boundaries. The energy components of the grain boundary energy are obtained from the sum of an integral of a local energy density and a pairlike term. This energy density is determined from the energy density of a homogeneous metal whose atom density is the same as the local atom density at each point in the boundary. Since homogeneous-metal-energy densities are quite easy to obtain as a function of atom density and can be tabulated, this part of the calculation is simple. The rest of the total energy is due to the pairlike interaction which is comparable in difficulty to the usual pair-potential calculation.

Thus we have a procedure in which the grain boundary is treated as a localized electronic defect from the outset. It will be interesting to find out how much improvement in computed grain boundary energies and structures ensues.

ACKNOWLEDGMENTS

The authors are indebted to A. Brokman for helpful comments and especially to R. W. Balluffi for suggesting this investigation and for advice throughout the course of the work. Helpful conversations with Dr. John Bradley, Dr. Robert Wagoner, Dr. Robert Ayres, Dr. Roy Richter, Dr. James Rose, and Dr. Jack Gay are acknowledged with thanks.

[1]See papers in J. Phys. (Paris) Colloq. **43**, C6 (1982).

[2]See papers in *The Nature and Behavior of Grain Boundaries*, edited by H. Hu (Plenum, New York, 1972).

[3]D. McLean, *Grain Boundaries in Metals* (Clarendon, Oxford, 1957).

[4]See papers in *Metal Interfaces* (American Society for Metals, Cleveland, Ohio, 1952).

[5]J. J. Croat, J. F. Herbst, R. W. Lee, and F. E. Pinkerton, J.

Appl. Phys. **55**, 2078 (1984).
[6]A. Brokman and R. W. Balluffi, Acta Metall. **29**, 1703 (1981).
[7]Thomas Kwok, Paul S. Ho, and Sidney Yip, Phys. Rev. B **29**, 5354 (1984).
[8]M. Hashimoto, Y. Ishida, R. Yamamoto, and M. Doyama, Acta Metall. **32**, 1 (1984).
[9]D. Wolf, Acta Metall. **32**, 245 (1984).
[10]P. D. Bristowe and A. Brokman, Scr. Metall. **14**, 1129 (1980).
[11]V. Heine and D. Weaire, in *Solids State Physics,* edited by H. Ehrenreich, F. Seitz, and D. Turnbull (Academic, New York, 1970), Vol. 24, especially p. 277. See also J. Hafner and V. Heine, J. Phys. F **13**, 2479 (1983).
[12]R. C. Pond and V. Vitek, Proc. R. Soc. London, Ser. B **357**, 453 (1979).
[13]Roy Richter, J. R. Smith, and J. G. Gay, *The Structure of Surfaces,* Vol. 2 of *Springer Series in Surface Science,* edited by M. A. Van Hove, and S. Y. Tong (Springer, Berlin, 1985), pp. 35–40; J. G. Gay, J. R. Smith, Roy Richter, F. J. Arlinghaus, and R. H. Wagoner, J. Vac. Sci. Technol. A **2**, 931 (1984); R. Richter, J. R. Smith, and J. G. Gay, Bull. Am. Phys. Soc. **29**, 264 (1984).
[14]John Ferrante and John R. Smith, Phys. Rev. B **19**, 3911 (1979); **31**, 3427 (1985).
[15]A. E. Carlsson, Phys. Rev. B **32**, 4866 (1985).
[16]E. G. Brovman and Yu. Kagan, Zh. Eksp. Teor. Fiz. **57**, 1329 (1969) [Sov. Phys.—JETP **30**, 721 (1970)].
[17]J. A. Moriarty, Phys. Rev. Lett. **55**, 1502 (1985).
[18]J. H. Rose, John Ferrante, and John R. Smith, Phys. Rev. Lett. **47**, 675 (1981).
[19]E. W. Müller and T. Z. Tsong, *Field Ion Microscopy* (American Elsevier, New York, 1969), p. 254.
[20]Y. Ishida, H. Ichinose, M. Mori, and H. Hashimoto, Trans. Jpn. Inst. Met. **24**, 349 (1983).
[21]J. Budai, W. Gaudig, and S. L. Sass, Philos. Mag. A **40**, 757 (1979).
[22]H. J. Frost and F. Spaepen, J. Phys. (Paris) Colloq. **43**, C6-73 (1982).
[23]R. C. Pond, D. A. Smith, and V. Vitek, Acta Metall. **27**, 235 (1979).
[24]D. A. Smith, V. Vitek, and R. C. Pond, Acta Metall. **25**, 475 (1977).
[25]P. D. Bristowe and A. G. Crocker, Philos. Mag. A **38**, 487 (1978).
[26]R. C. Pond and V. Vitek, Proc. R. Soc. London, Ser. A **357**, 453 (1977).
[27]Y. Ishida, H. Ichinose, and M. Mori, Proceedings of the 8th European Congress on Electron Microscopy, Budapest, Hungary, 1984 (unpublished).
[28]R. W. Balluffi and P. D. Bristowe, Scr. Metall. **18**, 617 (1984).
[29]W. Kohn and L. J. Sham, Phys. Rev. **140**, A1133 (1965).
[30]N. W. Ashcroft, Phys. Rev. **155**, 682 (1967).
[31]R. W. Shaw, J. Phys. C **2**, 2335 (1969).
[32]D. M. Wood and D. Stroud, Phys. Rev. B **28**, 4374 (1983). See also N. W. Ashcroft and D. Stroud, in *Solid State Physics,* edited by H. Ehrenreich, F. Seitz, and D. Turnbull (Academic, New York, 1978), Vol. 33, p. 2.
[33]Z. Wang and D. Stroud (private communication). These authors evaluated $E_2[n;\delta V(\mathbf{r})]$ for single-crystal aluminum using an Ashcroft pseudopotential (Ref. 27).
[34]The Hubbard dielectric function as modified by Geldart and Vosko was used [D. J. W. Geldart and S. H. Vasko, Can. J. Phys. **44**, 2137 (1966); see also P. Vashishta and K. S. Singwi, Phys. Rev. B **6**, 875 (1972); **6**, 883 (1972)].
[35]C. Kittel, *Introduction to Solid State Physics,* 4th ed. (Wiley, New York, 1971).
[36]L. E. Murr, Acta Metall. **21**, 791 (1973).
[37]G. F. Bolling, Acta Metall. **16**, 1147 (1968).
[38]J. H. Rose and J. F. Dobson, Solid State Commun. **37**, 91 (1981).
[39]S. C. Ying, J. R. Smith, and W. Kohn, Phys. Rev. B **11**, 1483 (1975).
[40]S. Chakravarty, J. H. Rose, D. Wood, and N. W. Ashcroft, Phys. Rev. B **24**, 1624 (1981).
[41]J. F. Dobson and J. H. Rose, J. Phys. C **15**, 7429 (1982).
[42]S. P. Singh and W. H. Young, J. Phys. F **3**, 1127 (1973).
[43]M. W. Finnis, J. Phys. F **4**, 1645 (1974).